Supplemental Materials

Molecular Biology of the Cell

Liu *et al*.

Supplemental Materials

Mff oligomerization is required for Drp1 activation and synergy with actin filaments during mitochondrial division

Ao Liu, Frieda Kage and Henry N. Higgs*

Department of Biochemistry and Cell Biology, Geisel School of Medicine at Dartmouth College, Hanover NH 03755, USA

*Correspondence. henry.higgs@dartmouth.edu

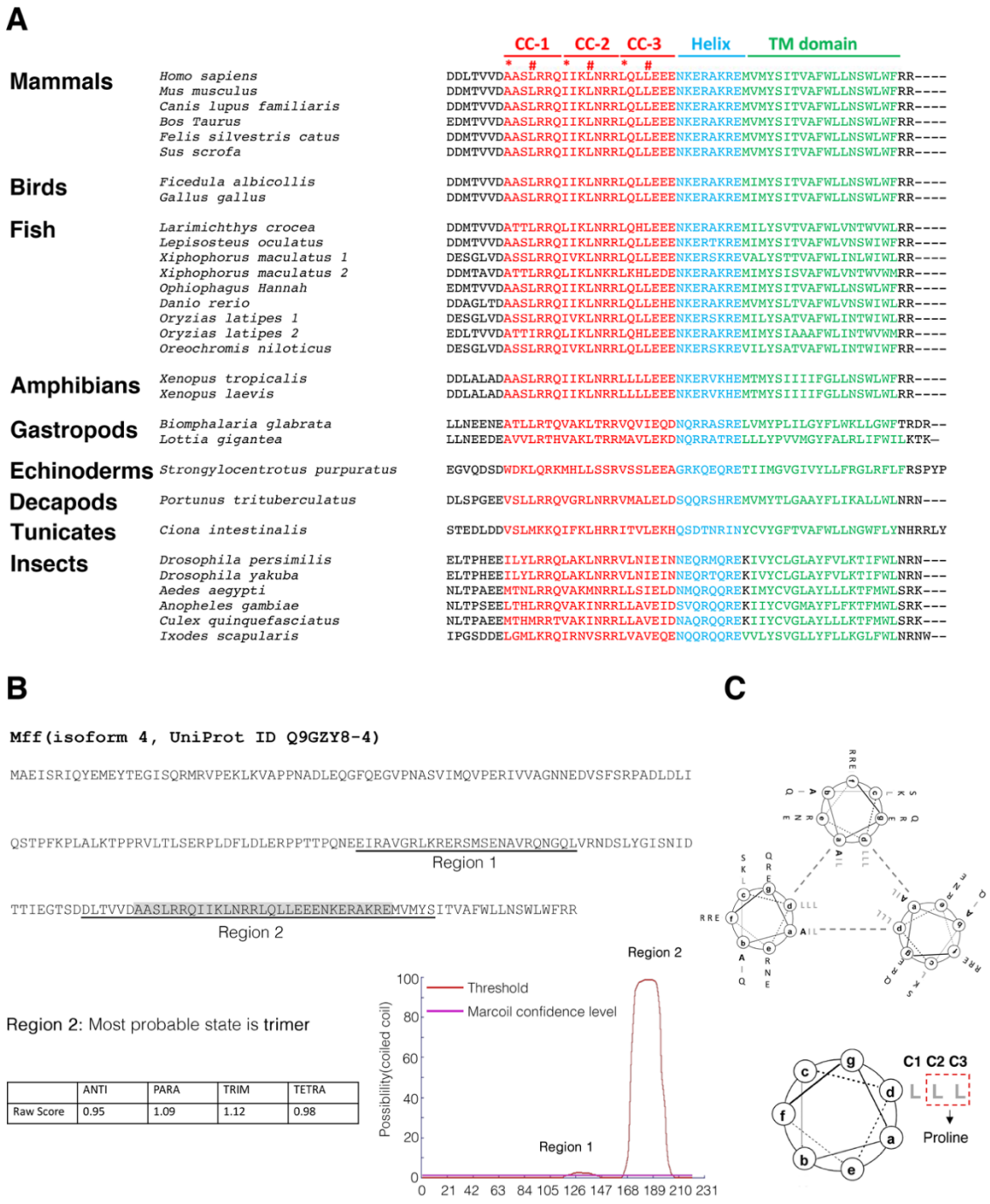

Figure S1. The coiled-coil region of Mff. A) Alignment of C-terminal region of Mff from a range of metazoans, showing the three heptad repeats of the coiled-coil (CC-1, 2 and 3), the helix region, the TM domain, and the short sequence in the inter-membrane space. A and D positions of the heptads shown with * and #, respectively. Sequence starts at amino acid 169 of human Mff isoform 0000. B) Analysis of

coiled-coil regions of Mff using LOGICOIL (Vincent *et al.*, 2013). Sequences of full length Mff is on the top (isoform 4, UniProt ID Q9GZY8-4). Underline indicates two possible predicted coiled-coil regions, grey box highlights the conservative coiled-coil in panel A. Scores of four possible coiled coil structures are predicted, positive score suggests high possibility. ANTI - anti parallel dimer, PARA - parallel dimer, TRIM - trimer, and TETRA - tetramer. C) Helical wheels for the Mff coiled-coil in a putative trimeric arrangement. To the bottom is illustrated the mutation of leucines in the D position of CC-2 and CC-3 to prolines to make the Mff-L2P construct (Chang *et al.*, 1999).

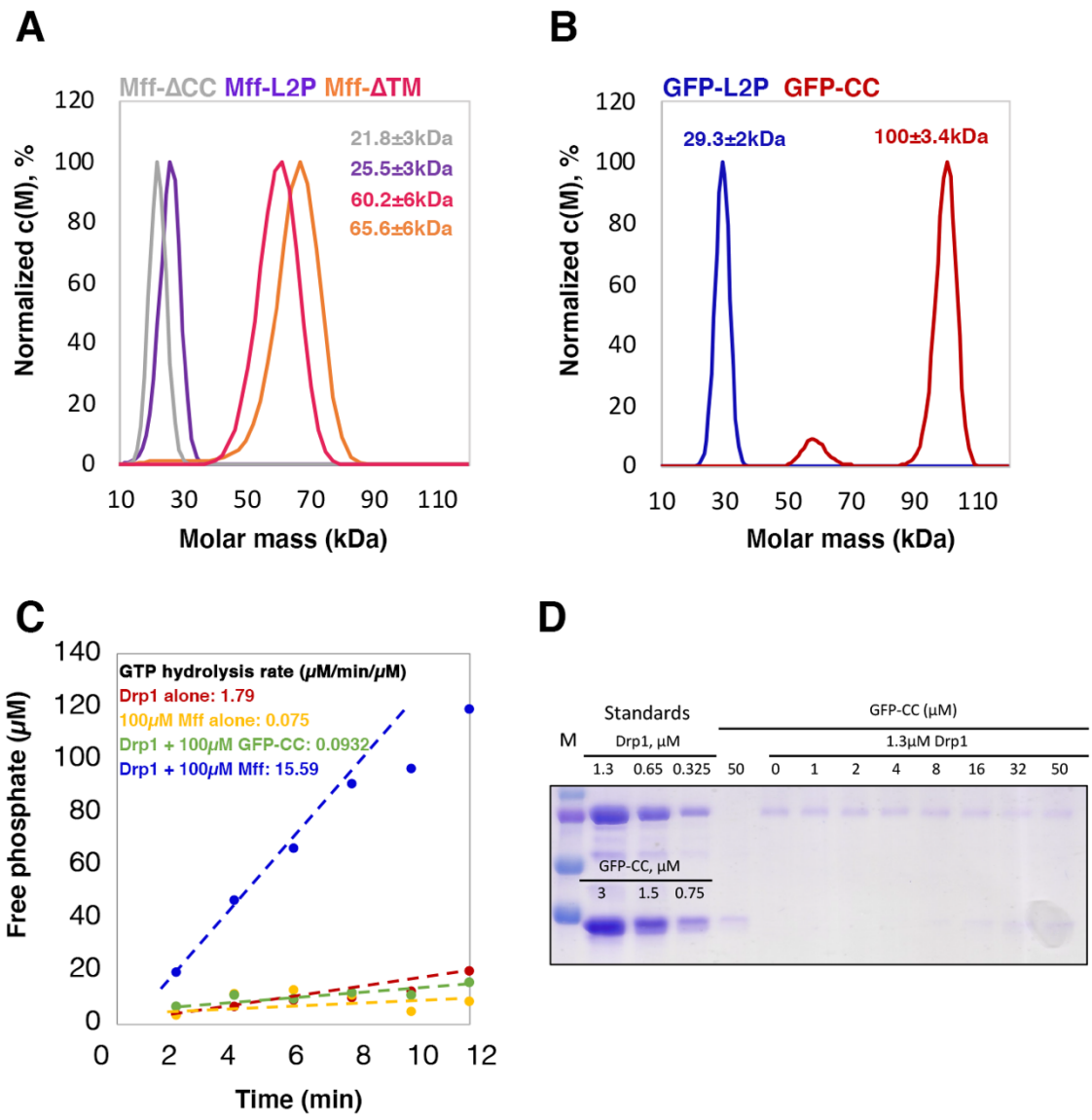

Figure S2. GFP-CC forms trimer and does not influence either Drp1 activity or its oligomerization. A) Velocity analytical ultracentrifugation of Mff-ΔTM at 100 μM (orange) or 250 μM (pink), and Mff-ΔCC (gray) or Mff-L2P (purple) at 100 μM. Y axis normalized to the peak c(M) for each sample, the maximum value of each curve is normalized as 100%. Peak masses listed on graph. B) Velocity analytical ultracentrifugation of 250 μM of GFP-CC (red) and GFP-L2P (blue). Peak molar mass prediction listed on graph. C) Time course of GTP hydrolysis by Drp1 alone (red), Mff alone (yellow), Drp1 + 100 μM GFP-CC (green), and Drp1 + 100 μM Mff (blue). D) High-speed pelleting assay of Drp1 (1.3 μM) in the presence GTP (1 mM) and of varying GFP-CC concentration. Drp1 and GFP-CC regions from the same SDS-PAGE

gel are presented. Standards equivalent to the indicated concentrations of Drp1 or GFP-CC in the assay on left of gels. Pellet fractions shown to the right.

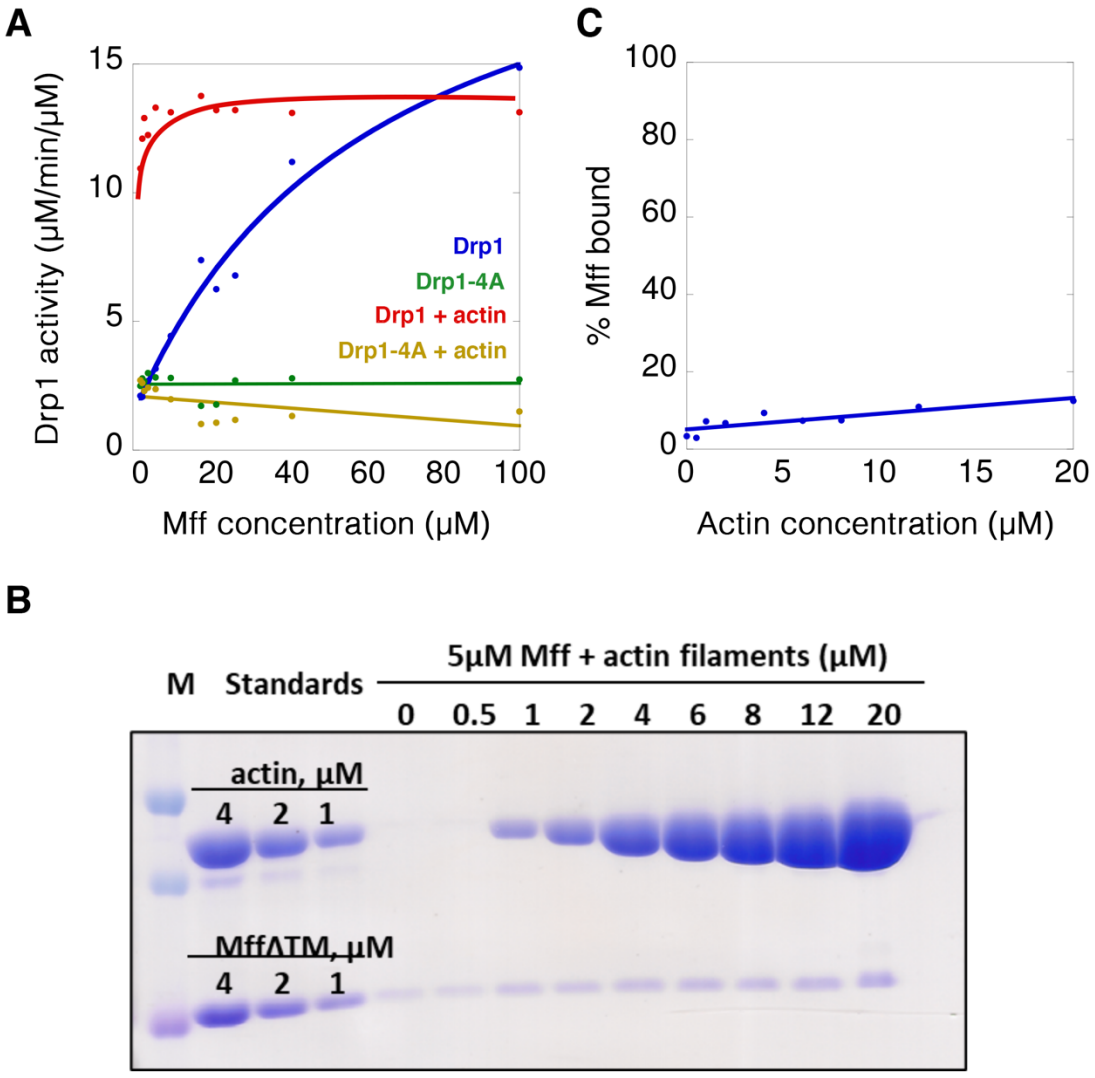

Figure S3. Mff-ΔTM does not directly interact directly with actin. A) GTPase activity of wild-type and oligomerization-defective mutant Drp1 401-404 AAAA (0.75 μM) as a function of Mff-ΔTM added, in the absence or presence of 0.5 μM actin filaments. B) High-speed pelleting assay of Mff-ΔTM (5 μM) in the presence of increasing concentrations of actin filaments. Standards equivalent to the indicated concentrations of Drp1 or Mff-ΔTM in the assay on the left. Pellet fractions shown to the right. C) Quantification of high-speed pelleting assay from panel B.

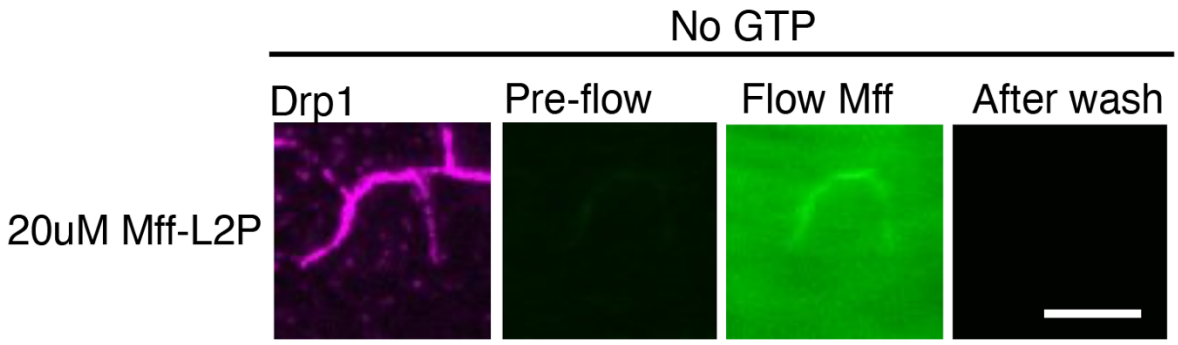

Figure S4. Binding of Mff-L2P to Drp1-bundled actin filaments at high concentration. TIRF assay conducted similarly to that in Figure 6D. Actin bundles were pre-formed with 0.1 μM actin (unlabeled, phalloidin-stabilized) and 2.5 μM Cy5-Drp1, then introduced into the TIRF chamber. Fluorescein-labeled Mff-L2P (20 μM) was introduced into the chamber in the absence of GTP while imaging. After 1 min, the chamber was washed while imaging. Bar, 10 μm.

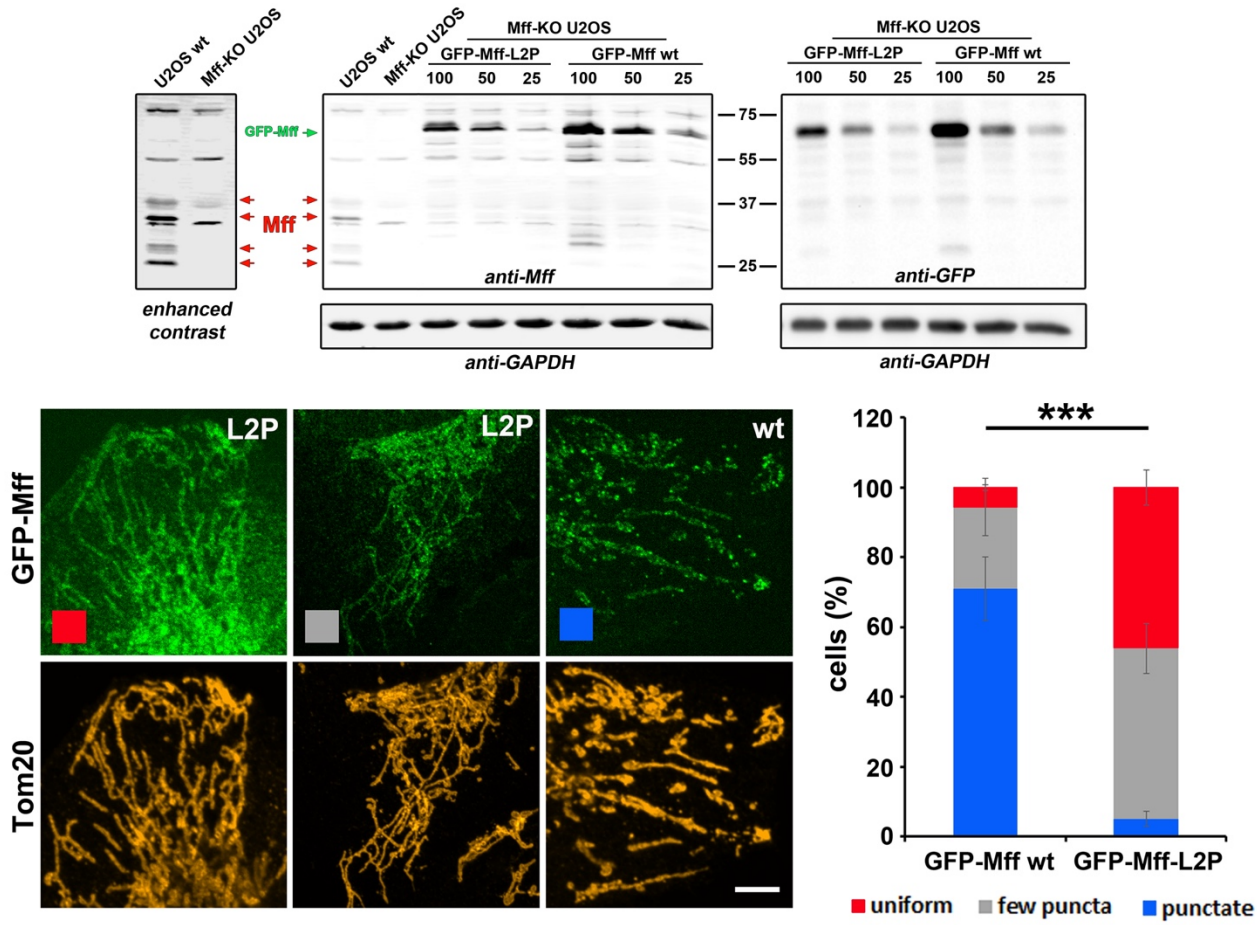

Figure S5. Expression and localization of GFP-fusion Mff constructs in Mff-KO U2OS cells. A) Western blots of cell extracts. Left and center blots are anti-Mff, with the left blot being an enhanced contrast version of a portion of the first two lanes of the center blot, showing that Mff KO results in disappearance of four bands (presumably corresponding to splice variants and/or post-translational modifications) but not of several background bands. Center blot shows change in anti-Mff signal for GFP-Mff with increasing amounts of plasmid transfected (in ng plasmid). Right blot shows anti-GFP of same transfected samples. Anti-GAPDH westerns are from the same blots. B) Examples of categories used for punctate GFP-Mff quantification in cells in panel C. Bar, 5 μm. C) Quantification of punctate nature of GFP-Mff mitochondrial localization, on Mff-KO U2OS cells transfected with either GFP-Mff-WT (25 ng plasmid) or GFP-Mff-L2P (50 ng plasmid), then fixed and stained for outer mitochondrial membrane with anti-Tom20. Data from 3 independent experiments, with 142 and 163 cells analyzed for GFP-Mff-WT and GFP-Mff-L2P, respectively. ***, p value < 0.001.

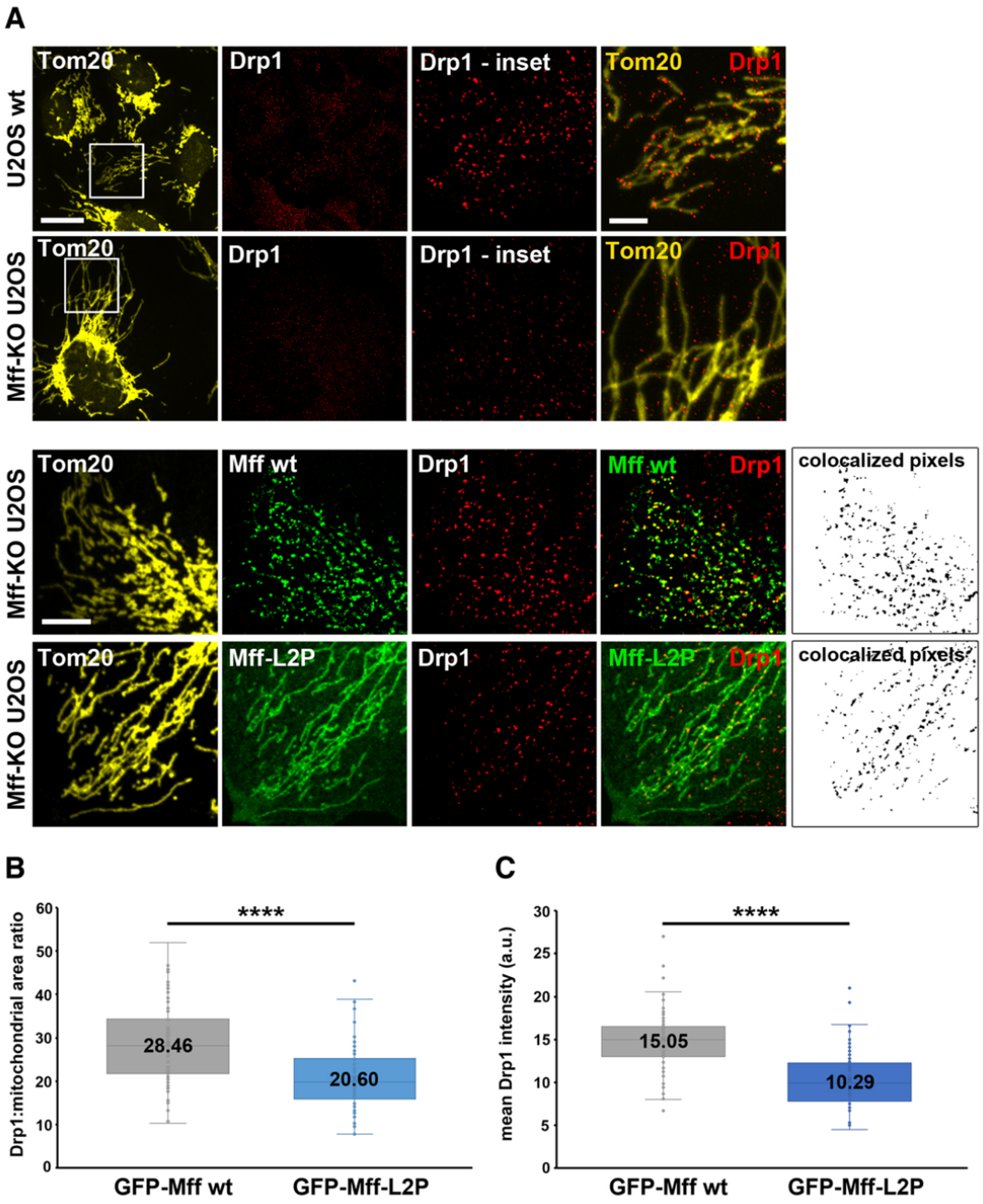

Figure S6. Distribution of Drp1 in Mff-KO U2OS cells expressing GFP-Mff constructs. A) Images of endogenous Drp1 distribution upon GFP-Mff expression in Mff-KO U2OS cells. Cells were transfected with either GFP-Mff-WT (25 ng plasmid) or GFP-Mff-L2P (50 ng plasmid), then fixed and stained with anti-Tom20 and anti-Drp1. Controls are untransfected WT and Mff-KO U2OS cells. Right-most image shows Drp1-stained pixels that co-localize with Tom20. Bars, 20 μm in overviews and 5 μm in insets. B) Quantification of area of mitochondrial Drp1 puncta as a function of mitochondria area from micrographs such as in panel A. ****, $p < 0.0001$. Numbers represent mean values. C) Quantification of mean Drp1 intensity per puncta, from micrographs such as in panel A. ****, $p < 0.0001$. 83 and 82 cells analyzed for Mff-WT and Mff-L2P, respectively.

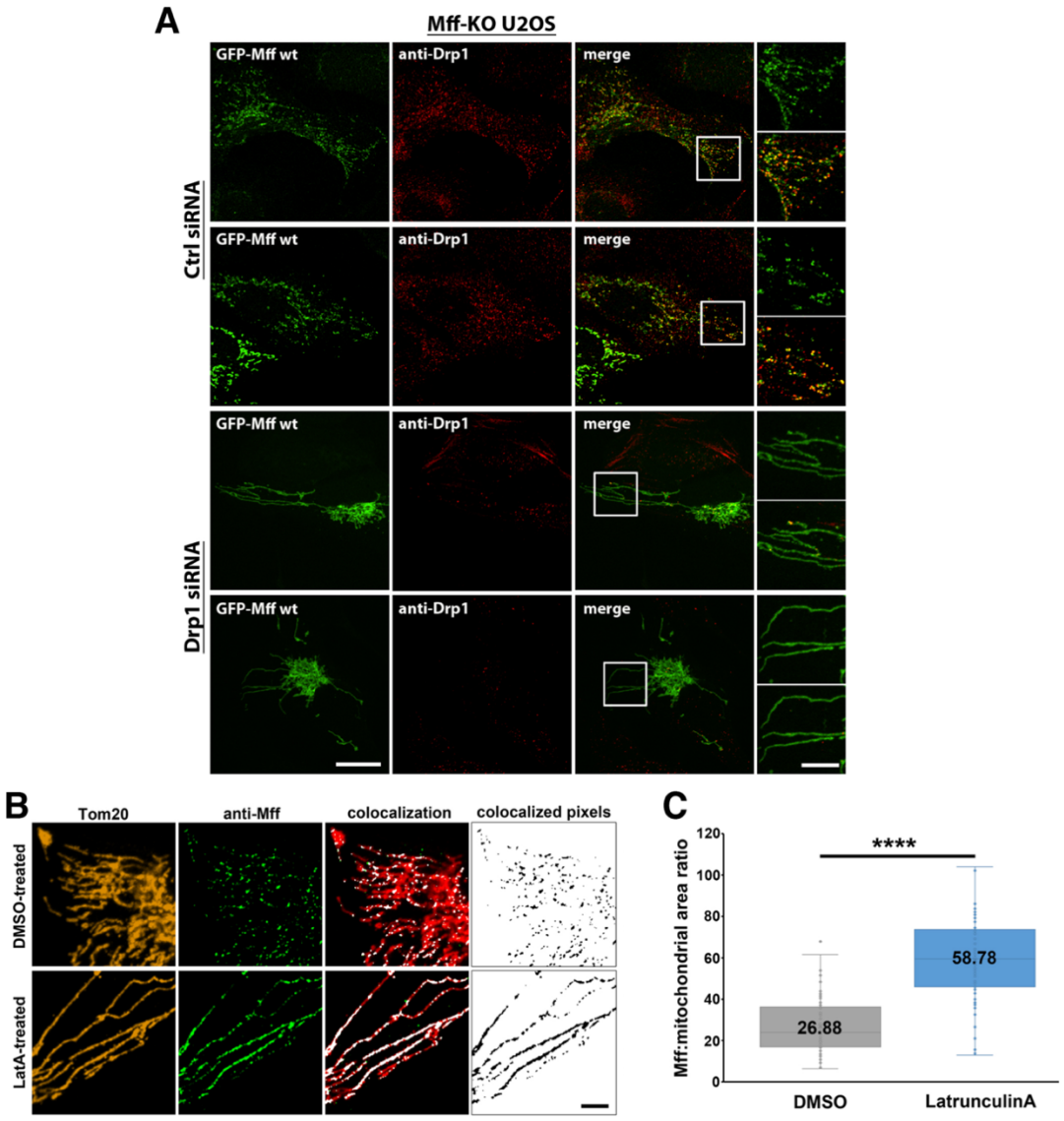

Figure S7. Effects of Drp1 and actin on cellular Mff puncta. A) Mff-KO U2OS cells were subjected to either control knock-down (top) or Drp1 knock-down (bottom) for 72 hrs, then transfected with GFP-Mff-WT (25 ng plasmid) for 24 hrs. Cells were fixed and stained with anti-Drp1. Two examples from control KD and Drp1 KD shown. Note long mitochondria and low anti-Drp1 staining in Drp1 KD cells, indicative of siRNA efficacity. B) Examples of WT U2OS cells treated with either DMSO (top) or 2 μM LatA (bottom) for 15 min before fixation and staining with anti-Tom20 and anti-Mff. Right-most images show the patterns of Mff staining on mitochondria. C) Quantification of mitochondrial area covered by Mff, as judged by the ratios of the mitochondrial Mff staining versus total mitochondrial staining from micrographs as in panel B. ****, $p < 0.0001$. 85 and 89 cells analyzed for DMSO and LatA, respectively.

Table S1 Hydrodynamic parameters of Mff and GFP by vAUC.

	Mff				GFP	
	250 μM	100 μM			250μM	
	Mff-ΔTM	Mff-ΔTM	Mff-ΔCC	Mff-L2P	GFP-CC	GFP-L2P
S value	3.03 ± 0.22	2.72 ± 0.171	1.21 ± 0.104	1.44 ± 0.136	4.89 ± 0.106	2.67 ± 0.134
Molecular Mass (kDa)	59.6 ± 6.4	65.6 ± 5.8	21.8 ± 2.7	25.5 ± 0.35	100.3 ± 3.4	29.3 ± 2
Frictional ratio	1.7133	2.036175	2.19496	2.044859	1.58723	1.279531
rmsd	0.005875	0.01225	0.021506	0.006419	0.007212	0.008566

*S value is defined as mean ± standard deviations.